HHS Public Access

Author manuscript

Multimodal Brain Image Anal (2012). Author manuscript; available in PMC 2015 July 21.

Published in final edited form as:

Multimodal Brain Image Anal (2012). 2012 January 1; 7509: 147–156. doi: 10.1007/978-3-642-33530-3_12.

Automatic Population HARDI White Matter Tract Clustering by Label Fusion of Multiple Tract Atlases*

Yan Jin[1], **Yonggang Shi**[1], **Liang Zhan**[1], **Junning Li**[1], **Greig I. de Zubicaray**[2], **Katie L. McMahon**[2], **Nicholas G. Martin**[3], **Margaret J. Wright**[3], and **Paul M. Thompson**[1]

Yan Jin: yjin@loni.ucla.edu; Yonggang Shi: yshi@loni.ucla.edu; Liang Zhan: lzhan@loni.ucla.edu; Junning Li: jli@loni.ucla.edu; Greig I. de Zubicaray: greig.dezubicaray@uq.edu.au; Katie L. McMahon: katie.mcmahon@uq.edu.au; Nicholas G. Martin: nick.martin@qimr.edu.au; Margaret J. Wright: margiew@qimr.edu.au; Paul M. Thompson: thompson@loni.ucla.edu

[1]Laboratory of Neuro Imaging, Department of Neurology, David Geffen School of Medicine, University of California, Los Angeles, Los Angeles, CA 90095, USA

[2]University of Queensland, Brisbane St. Lucia, QLD 4072, Australia

[3]Queensland Institute of Medical Research, Herston, QLD 4029, Australia

Abstract

Automatic labeling of white matter fibres in diffusion-weighted brain MRI is vital for comparing brain integrity and connectivity across populations, but is challenging. Whole brain tractography generates a vast set of fibres throughout the brain, but it is hard to cluster them into anatomically meaningful tracts, due to wide individual variations in the trajectory and shape of white matter pathways. We propose a novel automatic tract labeling algorithm that fuses information from tractography and multiple hand-labeled fibre tract atlases. As streamline tractography can generate a large number of false positive fibres, we developed a top-down approach to extract tracts consistent with known anatomy, based on a distance metric to multiple hand-labeled atlases. Clustering results from different atlases were fused, using a multi-stage fusion scheme. Our “label fusion” method reliably extracted the major tracts from 105-gradient HARDI scans of 100 young normal adults.

1 Introduction

Diffusion tensor magnetic resonance imaging (DT-MRI) recovers the local profile of water diffusion in tissues, yielding information on white matter (WM) integrity and connectivity that is not available from standard anatomical MRI. Recently, DT-MRI has been extended to more sophisticated models of the local diffusion process, such as high angular resolution diffusion imaging (HARDI [1]) and diffusion spectrum imaging. These advances allow more accurate reconstruction of fibres that mix and cross. WM fibres may be recovered using tractography methods that fit a path through the directional diffusion data at each voxel. Due to its speed, the streamline technique has been extensively used for whole-brain tractography. Streamline methods follow the principal eigenvector in DT-MRI [2] or the

*This study was supported by Grant RO1 HD050735 from the National Institutes of Health (NIH) and Grant 496682 from the National Health and Medical Research Council (NHMRC), Australia.

dominant directions extracted from orientation distribution functions (ODF) [1] in HARDI to trace out a fibre trajectory in 3D.

Clustering methods can group the fibres from tractography, enabling large population studies of disease and genetic effects on tract shapes, or tract integrity. Various approaches have been proposed for automatically clustering fibres. One simple strategy selects anatomically well-known WM tracts that are "seeded" in regions of interest (ROI) [3]. One problem with this approach is that ROIs either have to be manually drawn on the scans, or must heavily rely on accurate registration of the scans to a previously labeled atlas. Image quality inevitably affects streamline tractography results, so many propagated streamlines fall short of reaching the ROIs and may be incorrectly excluded from the resulting tracts.

A typical framework for fibre clustering defines a pairwise similarity/distance between each pair of fibres in a large set of candidate fibres, to group them into separate and distinct tracts. The resulting similarity matrix (that compares all fibres with all others) can serve as the input for standard clustering algorithms [4]. It is difficult for a user to specify the number of clusters or a threshold to decide when to stop merging or splitting clusters. Clustering results vary drastically when different numbers of clusters are chosen. Without any anatomical information to guide the clustering, tracts may not correspond to any anatomically familiar subdivisions. Some recent work [5-6] has addressed this problem by adding atlas information into the framework. However, whole-brain tractography typically produces 10,000-100,000 fibres per subject. These "bottom-up" methods (clustering individual fibres into larger and larger groups until major tracts are aggregated) can fail to filter out the large number of erroneous fibres generated by streamline methods.

To group fibres into coherent tracts that are consistently labeled across a population, a labeled training dataset (atlas) can be used. In traditional image segmentation, a deformable atlas may be used, in which an expertly labeled atlas is non-rigidly registered to the image to be segmented. The resulting deformation can then be used to transfer the training labels onto the test image. Recently, *label fusion* became popular for registration-based image segmentation [7-8]. Multiple atlases and registrations are used to transfer multiple training labels to the test subject space. The final labeling is obtained by applying a weighting strategy to the labels transferred from different atlases. Label fusion has two advantages: (1) large individual variations in anatomy can be better accommodated if one does not need to rely on a single atlas; (2) multiple registrations improve robustness against occasional registration failures, and non-global minima of the registration cost function.

Here we introduce a *multi-atlas label fusion* framework to automatically extract anatomically meaningful WM tracts. By organizing the results of whole-brain tractography into familiar and recognizable tracts, we provide a robust clustering of fibres for population studies. Based on the ROIs from a publicly available parcellated WM atlas [9], we first manually construct a number of WM fibre tract atlases, each consisting of a set of several major WM tracts. In contrast to prior "bottom-up" methods, we use the WM tracts in multiple hand-labeled atlases as prior anatomical information. Our "top-down" approach transfers tract labels by selecting only fibres that are similar to the corresponding tracts in the atlases, based on a similarity measure. This eliminates many false positive fibres that

may be otherwise hidden in the ∼100,000 fibres per subject produced by streamline tractography. Multiple atlases help to adapt to the variability of tract shapes in new subjects, and further reduce the number of outliers arising from registering a single atlas to diffusion images or to whole-brain tractography from a new subject. Finally, we use a multi-stage fusion scheme to fuse the clustered results obtained from individual atlases. A workflow diagram is shown in Figure 1. To test the robustness of our algorithm, we applied it to a population study over 100 HARDI datasets.

2 Label Fusion Clustering Framework

2.1 Data Acquisition

Our 100 subjects were selected from a much larger database of ∼700 healthy young adult twins in their twenties from Australia. They were all right-handed. HARDI images were acquired with a 4-Tesla Bruker Medspec MRI scanner. Each 3D volume consisted of 55 2-mm axial slices and 1.79×1.79mm^2 in-plane resolution with 128×128 acquisition matrix. 105 image volumes were acquired per subject: 11 with T2-weighted b0 images and 94 diffusion-weighted volumes (b = 1159 s/mm^2). We only used unrelated subjects in this analysis, leaving genetic analysis to future work.

2.2 Tractography

Raw HARDI images were corrected for eddy-current induced distortions with FSL (http://www.fmrib.ox.ac.uk/fsl/). We performed the whole-brain tractography with Camino (http://cmic.cs.ucl.ac.uk/camino/), an open source software package that uses both streamline and probabilistic algorithms to reconstruct fibre paths. The spherical harmonic (SH) representation provides faster ODF estimation, and is more robust to noise and arguably more accurate for detecting fibre crossings than the original numerical *q*-ball reconstruction method [10]. Explicitly, the SH basis may be expressed as follows:

$Y_l^m(\theta,\varphi)=\sqrt{\frac{(2l+1)(l-m)!}{4\pi(l+m)!}}P_l^m(\cos\theta)e^{im\varphi}$, where *l* denotes the order, *m* denotes the phase factor, $\theta\in[0,\ \pi]$, $\phi\in[0,2\pi]$, and P_l^m is an associated Legendre polynomial. Signal at each gradient direction may be approximated as a linear combination of a modified version of this SH basis. We used the 6th order (*l*=6) SH series to reconstruct ODFs for our HARDI data and a maximum of 3 local ODF maxima (where fibres mix or cross) were set to be detected at each voxel. Streamline tractography followed these principal diffusion directions with the Euler interpolation method to generate fibres inside the entire brain. The maximum fibre turning angle was set to 35°/voxel, and tracing stopped at any voxel whose fractional anisotropy (FA) <0.2.

2.3 WM Tract Atlas Construction

We constructed four WM tract atlases, from the healthy twins' HARDI data acquired as in **Section 2.1**. A single-subject template in the ICBM-152 space called the “Type II Eve Atlas” (a 32-year old healthy female) [9] were registered to the FA images of each atlas. The entire brain of the “Eve” template was previously parcellated using 130 bilateral ROIs.

Linear and then non-linear registration was performed with Advanced Normalization Tools (ANTs) [11].

The labeled template ROIs were re-assigned to the four registered atlases, respectively, by warping them with the deformation fields generated by ANTs. Fibres that traversed the ROIs were extracted according to the lookup table in [12]. For example, the corticospinal tract was extracted from fibres passing between the precentral gyrus and the cerebral peduncle. Each tract was manually edited to remove visible outliers and to add any short fibres that incorrectly failed to reach the ROIs. Guevara *et al*. [13] used a single multi-subject atlas in their clustering algorithm. In principle, multiple atlases should be more robust to inaccuracies in registration.

Currently, each atlas is comprised of 13 major WM tracts: the left/right corticospinal tracts, left/right *cingulum*, left/right arcuate fasciculi (part of the superior longitudinal fasciculi), left/right inferior fronto-occipital/longitudinal fasciculi, and five segments of the corpus callosum – projecting to both frontal lobes, precentral gyri, postcentral gyri, superior parietal lobes, and the occipital lobes. We combined the inferior fronto-occipital fasciculus and inferior longitudinal fasciculus as one tract, as they had substantial overlap during manual atlas construction due to tractography and our image quality.

Figure 2 shows an example WM tract atlas that we created (*top*, *left side*, and *back* views).

2.4 Fibre Clustering

For each test subject (i.e., each new dataset to be labeled), whole-brain tractography was extracted using Camino as well. The same registration registered the subject's FA image to each of the four WM tract atlases' FA images, respectively. Each atlas's tracts were then warped to the subject space with the corresponding deformation fields generated from the FA registration. Ideally, an ODF-based registration method should be used to reorient the fibres between different spaces. However, such a registration scheme would have tremendous costs in terms of time (a few hours per registration) and computing resources if it were performed on a large-scale, as in the label fusion scheme. In contrast, FA registration only takes 5 minutes per registration on our datasets. Moreover, it has also been shown that fibre alignment is indeed improved significantly with that type of registration [14]. The use of multiple atlases also helps to reduce clustering errors due to imperfect registration.

We defined a fibre distance metric to decide the subject's fibres that should be included in any individual warped atlas tract, based on an empirical threshold obtained from our training data. For any pair of fibres γ_i and γ_j, we define the symmetric Hausdorff distance: $d_H(\gamma_i,\gamma_j) = \max(d_{H'}(\gamma_i,\gamma_j), d_{H'}(\gamma_j,\gamma_i))$, where $d_{H'}$ is the asymmetric Hausdorff distance. $d_{H'}(\gamma_i,\gamma_j) = max_{x\in\gamma i}\, min_{y\in\gamma j}\, \|x-y\|$. $\|\cdot\|$ is the Euclidean norm and the ordered pair (γ_i,γ_j) indicates an asymmetric distance from γ_i to γ_j. x's and y's are the coordinate points along fibres γ_i and γ_j, respectively [4].

For each fibre that belonged to a particular tract in an atlas, we computed the distance between this fibre and each fibre in the subjects' tractography that traversed within a

neighborhood around the points along this atlas fibre. For a particular atlas, a group of the subject's fibres was identified as the clustering result for each atlas tract.

2.5 Multi-stage Label Fusion

To correctly fuse all the candidate fibres we obtained in **Section 2.4**, there are two pieces of information we need to consider: the position/geometric shape of the fibre, and the similarity between the atlases and the subject.

Majority Voting—We chose the Hausdorff distance metric in the fibre clustering phase because streamline tractography produces many false positives and this metric is relatively conservative in terms of including outliers. It will only pick streamlines with the similar geometric shapes that lie in the region where the particular atlas WM tract is located. However, due to the WM variability of individual atlases, they may nominate different candidates based on their own tract shapes. Majority voting, although it is probably the simplest label fusion method, has been proven to yield accurate segmentation results [15]. We decided that if a fibre appeared in at least 2 out of 4 individual clustering results, we considered it to be a true fibre that should be considered in the next step; otherwise, it was discarded.

Similarity of the Atlas to the Subject—The degree of correspondence between the atlas and the subject is another factor that should be taken into account. One way to measure it is to evaluate the registration quality locally along the candidate fibre. We first warped each candidate fibre that passed majority voting to the corresponding atlases (those who picked it out) with the inverse deformation fields generated by FA registration in Section 2.4. Then the angle between the fibre direction at each point on the warped fibre and the dominant direction of the ODF at the same point in the atlas was calculated. Camino uses the Euler method to interpolate fibre points. Therefore, the fibre direction is defined as: $(\vec{x_{i+1}}-\vec{x_i})/\|\vec{x_{i+1}}-\vec{x_i}\|$, i=1,…,$n$-1, where $\vec{x_i}$ is the point on the fibre, n is the number of points on the fibre, and $\|\cdot\|$ is the magnitude of the vector. The atlas ODF direction is the 3D linearly interpolated vector obtained through the closest ODF peak directions found in tractography at the 8 neighboring voxels. For each voxel, there may be multiple peak directions detected in tractography, so we picked the one or its 180° opposite that has the smallest subtended angle (that is, the largest inner product) from the fibre direction as the closest ODF peak direction at this voxel. A 3D linear interpolation was then used to find the ODF direction at the specified fibre point location. We calculated the percentage of the angles that were smaller than a threshold (for example, we used 25°) among all the points on that fibre and averaged it over all the atlases that chose the fibre for a particular tract. If the overall percentage was above a threshold (for example, 80%), we considered the overall registration quality to be good. The fibre picked out by those atlases was reliable and should be labeled as being part of that tract; otherwise, it was discarded. Figure 3 illustrates a good and a bad local registration based on our criterion.

3 Results

3.1 Automatic Clustering Results

Figure 4 shows how we obtain the left inferior fronto-occipital/longitudinal fasciculus (in *green*) in a test subject. The first row shows the four atlas versions of the tract. The second row shows the four different candidates for this tract in the same test subject, based on using each atlas to decide which fibres it should contain. We used the Hausdorff distance (see Section 2.4) with the threshold of 10mm to find potential fibre candidates. The final result for this tract was obtained by applying the label fusion scheme in Section 2.5. It is not hard to see that the label fusion process can help to eliminate outliers or add missing fibres in a single candidate. Figure 5 shows the label fusion results for the right cingulum (in *cyan*) in four *different* subjects. Despite individual variations, the overall tract shapes are consistent across the population. Figure 6 shows automatic WM fibre clustering results for two representative test subjects. Top, left side, and back views are shown. The types of tracts and their colors are as in Figure 1. The average fibre number in our clustering results is ∼10,000 per subject, a 1 in 10 data reduction relative to the initial tractography.

3.2 Population-Based Statistical Results

Many analyses are possible on these clustered tracts, for example, genetic analysis of fibre tract geometry, integrity, and connectivity. As one example of a typical application, we calculated the mean FA across all voxels traversed by specific tracts in 100 subjects, and tested for any differences in mean FA between the left and right hemispheres (Table 1). Interestingly, the mean FA of the left corticospinal tract is significantly higher than that of the right one. This is consistent with prior studies since all our subjects are right-handed, and there is a tendency towards a higher degree of myelination in tracts that control the right side of the body, at least in righthanders.

4 Discussion

Multiple atlases were used in our framework to capture the individual variability of tract shapes. However, optimal selection of the number of atlases in label fusion is still an open question; for our application we will perform convergence tests once we have sufficient ground truth data. The focus of this paper is to show the benefit of using multi-atlases (Fig. 4). Based on our data, four atlases already offer a reasonable number of tracts to account for the WM shape variability in our sample, relative to the time needed to build atlases by hand.

We empirically decided on the Hausdorff threshold (Section 2.4), and the angle and the percentage (Section 2.5) as similarity metrics, to help recover similar numbers of fibres in the test subjects versus atlases, based on our training data. Quantitative analysis would be more convincing, but without having ground truth at the moment, a meaningful comparison is not easily achieved; currently, we are working on creating many hand labelled datasets to serve as ground truth.

Validation of any particular clustering of real fibre tract data is difficult, as there is no agreed ground truth on what fundamental elements the connectivity pattern contains. It is very difficult to validate clustering quantitatively except by careful visual inspection, as it is

often clearer which fibres are false positives than true positives [4][6]. Clustering relies on fibres obtained from tractography, which is already tough to validate, except on phantoms, and phantoms may not be realistically complex. Comparing Dice coefficients between different approaches and hand-labeled tracts might be feasible and will be part of our future work, but is very time consuming. Instead, we show preliminary illustrations to indicate how label fusion can add missing fibres or delete obvious false positives, compared to a single atlas, in Fig. 4. We also used the FA statistics on the corticospinal tracts in **Section 3.2** to show that our method can pick up subtle known effects.

5 Conclusion

Here we presented an automatic fibre clustering pipeline that uses anatomical information from multiple manually made atlases. It can robustly segment the brain WM fibres into major tracts; we showed an illustrative example where we applied it to segment and cluster tracts in 100 subjects. The contribution of our work is to extend the well-established label fusion technique in atlas-based image segmentation to fibre clustering. This results in a powerful approach to large population studies in various neurological and psychiatric research fields, as well as in imaging genetics, where vast samples must be phenotyped to identify genes that affect brain integrity.

References

1. Tuch DS. Q-Ball Imaging. Magn Reson Med. 2004; 52:1358–1372. [PubMed: 15562495]
2. Mori S, Crain BJ, Chacko VP, van Zijl PC. Three-dimensional Tracking of Axonal Projections in the Brain by Magnetic Resonance Imaging. Ann Neurol. 1999; 45:265–269. [PubMed: 9989633]
3. Wakana S, Caprihan A, Panzenboeck MM, Fallon JH, Perry M, Gollub RL, Hua K, Zhang J, Jiang H, Dubey P, Blitz A, van Zijl P, Mori S. Reproducibility of Quantitative Tractography Methods Applied to Cerebral White Matter. NeuroImage. 2007; 36:630–644. [PubMed: 17481925]
4. O'Donnell LJ, Westin CF. Automatic Tractography Segmentation using a High-dimensional White Matter Atlas. IEEE Trans Med Imag. 2007; 26:1562–1575.
5. Maddah M, Zöllei L, Grimson WE, Westin CF, Wells WM. A Mathematical Framework for Incorporating Anatomical Knowledge in DT-MRI Analysis. 5th IEEE ISBI. 2008:105–108.
6. Wassermann D, Bloy L, Kanterakis E, Verma R, Deriche R. Unsupervised White Matter Fibre Clustering and Tract Probability Map Generation. NeuroImage. 2010; 51:228–241. [PubMed: 20079439]
7. Artaechevarria X, Munoz-Barrutia A, Ortiz-de-Solorzano C. Combination Strategies in Multi-Atlas Image Segmentation: Application to Brain MR Data. IEEE Trans Med Imag. 2009; 28:1266–1277.
8. Sabuncu M, Yeo BT, Van Leemput K, Fischl B, Golland P. A Generative Model for Image Segmentation Based on Label Fusion. IEEE Trans Med Imag. 2010; 29:1714–1729.
9. Oishi K, et al. Atlas-based Whole Brain White Matter Analysis using Large Deformation Diffeomorphic Metric Mapping. NeuroImage. 2009; 46:486–499. [PubMed: 19385016]
10. Descoteaux M, Faria A, Jiang H, Li X, Akhter K, Zhang J, Hsu JT, Miller MI, van Zijl PC, Albert M, Lyketsos CG, Woods R, Toga AW, Pike GB, Rosa-Neto P, Evans A, Mazziotta J, Mori S. Regularized, Fast and Robust Analytical Q-ball Imaging. Magn Reson Med. 2007; 58:497–510. [PubMed: 17763358]
11. Avants BB, Tustison NJ, Song G, Cook PA, Klein A, Gee JC. A Reproducible Evaluation of ANTs Similarity Metric Performance in Brain Image Registration. NeuroImage. 2011; 54:2033–2044. [PubMed: 20851191]
12. Zhang Y, Zhang J, Oishi K, Faria AV, Jiang H, Li X, Akhter K, Rosa-Neto P, Pike GB, Evans A, Toga AW, Woods R, Mazziotta JC, Miller MI, van Zijl PC, Mori S. Atlas-Guided Tract

Reconstruction for Automated and Comprehensive Examination of the White Matter Anatomy. NeuroImage. 2010; 52:1289–1301. [PubMed: 20570617]

13. Guevara P, Duclap D, Poupon C, Marrakchi-Kacem L, Fillard P, Le Bihan D, Leboyer M, Houenou J, Mangin JF. Automatic Fibre Bundle Segmentation in Massive Tractography Datasets using a Multi-subject Bundle Atlas. 14th MICCAI Workshop on CDMRI. 2011
14. Jin Y, Shi Y, Jahanshad N, Aganj I, Sapiro G, Toga AW, Thompson PM. 3D Elastic Registration Improves HARDI-derived Fibre Alignment and Automated Tract Clustering. 8th IEEE ISBI. 2011:822–826.
15. Rohlfing T, Brandt R, Menzel R, Maurer CR Jr. Evaluation of Atlas Selection Strate-gies for Atlas-based Imaging Segmentation with Application to Confocal Microscopy Images of Bee Brains. NeuroImage. 2004; 21:1428–1442. [PubMed: 15050568]

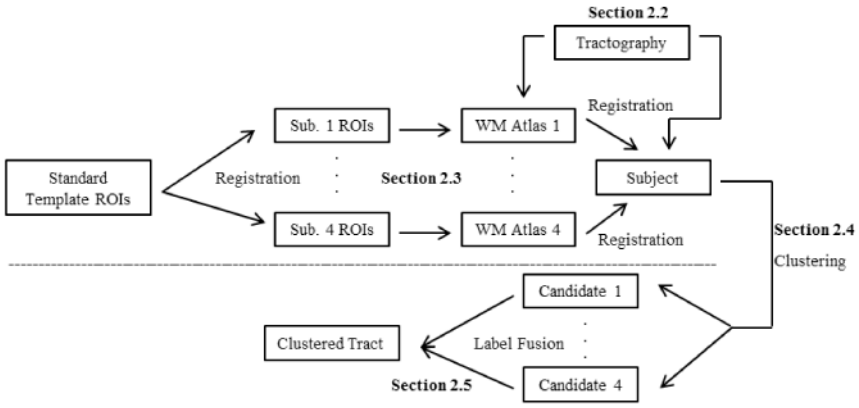

Fig. 1. A flow chart showing steps in our label fusion algorithm for clustering fibres

Fig. 2.

A representative WM fibre atlas computed, and manually edited, from 4-Tesla 105-gradient HARDI data, showing major tracts. *Top*, *left side*, and *back* views are shown. Major tracts, distinguished in color, include the corticospinal tracts (*deep sky blue*), the cingulum on each side (*cyan*), arcuate fasciculi (*blue*), inferior fronto-occipital/longitudinal fasciculi (*green*), and multiple subdivisions of the corpus callosum (warm colors from *red* to *yellow*).

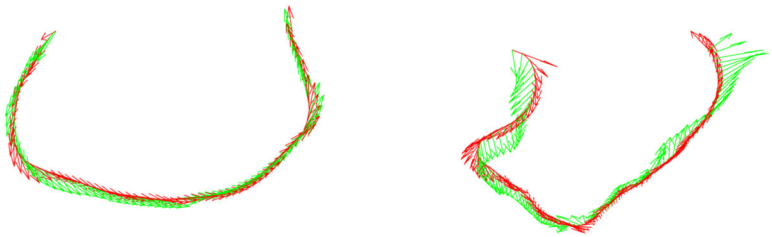

Fig. 3.

This illustration shows the quality of the matching between the fibre direction of the subject and the local ODF principal direction of the atlas. A good match of a corpus callosum fibre is shown on the left and a poor match of another corpus callosum fibre is shown on the right (the fibre direction is in *red* and the ODF direction is in *green*).

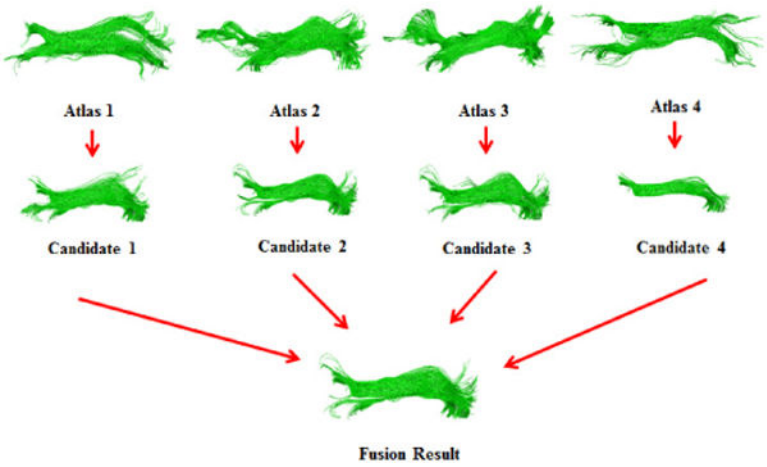

Fig. 4. Label fusion result for the left inferior fronto-occipital/longitudinal fasciculus (in *green*) in a test subject (viewed from the *left*)

Fig. 5. Label fusion result for the right cingulum (in *cyan*) in four *different* subjects (viewed from the *left*)

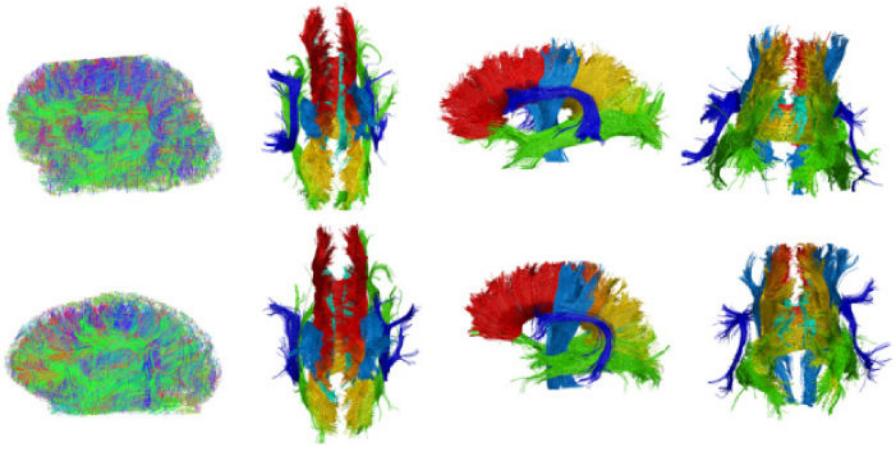

Fig. 6.

Results of automatic fibre clustering, for two subjects. For the tract names and colors used to distinguish them, please see Fig. 1 (view from *top*, *left side*, and *back*, respectively). The leftmost column is the original whole-brain tractography, for comparison.

Table 1

Population analysis of asymmetry in FA for various tracts, in 100 subjects.

Tract Name	Mean FA (Left/Right)		*p*-value
Corticospinal	0.4644	0.4528	$^{*}1.15\times10^{-12}$
Inferior fronto-occipital	0.4501	0.4544	$^{*}0.01$
Cingulum	0.4107	0.4034	$^{*}7.30\times10^{-5}$
Arcuate fasciculus	0.4623	0.4566	0.06

* indicates that the difference is statistically significant.